



PERGAMON

Solid State Communications 122 (2002) 553–556

solid  
state  
communications

[www.elsevier.com/locate/ssc](http://www.elsevier.com/locate/ssc)

## Engineering vertically aligned InAs/GaAs quantum dot structures via anion exchange

Y.Q. Wang<sup>a</sup>, Z.L. Wang<sup>a,\*</sup>, J.J. Shen<sup>b</sup>, A.S. Brown<sup>b\*</sup>

<sup>a</sup>*School of Materials Science and Engineering, Georgia Institute of Technology, Atlanta, GA 30332-0245, USA*

<sup>b</sup>*School of Electrical and Computer Engineering, Georgia Institute of Technology, Atlanta, GA 30332, USA*

Received 17 March 2002; accepted 16 April 2002 by D. Van Dyck

### Abstract

P/As anion exchange is exploited to modify stacked InAs/GaAs quantum dot structures grown by molecular beam epitaxy (MBE). It is shown that the vertical alignment and size uniformity can be remarkably improved via P/As anion exchange. This, therefore, demonstrates a promising approach to tuning the quantum dot morphologies and structures, and hence, the electronic and optoelectronic properties. © 2002 Elsevier Science Ltd. All rights reserved.

PACS: 81.07.Ta

Keywords: A. Self-assembling; B. InAs quantum dot; C. Anion exchange; D. Stranski–Krastanov (S–K) growth

Self-assemble by exploiting the Stranski–Krastanov (S–K) growth of highly lattice-mismatched semiconductors is widely recognized as a powerful technique for fabrication of semiconductor quantum dot structures for novel electronic and optoelectronic applications [1,2]. In the S–K growth mode, coherent islands are formed through a spontaneous nucleation and growth process, which is fundamentally based on surface morphological instability driven by relaxation of the strain energy in lattice-mismatched heterostructures. This in situ growth process offers advantages in comparison to ex situ techniques, such as lithography. However, the spontaneous nature of the S–K growth generally produces islands distributed randomly and with a distribution of island sizes. This size non-uniformity causes considerable broadening of optical transition energies and poses a serious limitation to device applications.

In multilayer structures, or quantum dot superlattices, it has been shown that the buried dots influence the nucleation and growth of the islands in subsequent layers, thereby giving rise to vertical alignment in the growth direction with improved size uniformity [3–6]. However, practically the

optimization of growth parameters to realize perfect vertical alignment and improved size uniformity of islands in stacked quantum dot structures is difficult. Factors, such as growth interruption, growth temperature, growth rate, and spacer layer thickness, can remarkably influence the vertical alignment and size uniformity [7–9]. It has been widely observed that the island size tends to increase in the upper dot layers, although the vertical alignment is well controlled [3,8,10,11].

We have been investigating the modification of quantum dot size, composition, strain, and optical properties via changes in growth conditions and the use of dissimilar anion anneal steps after formation of the dots. In our anion exchange approach, the InAs quantum dots are annealed under a P<sub>2</sub> flux. Previous work has shown that (1) P-for-As anion exchange, or intermixing of P and As in the top surface InAs layer, occurs during P<sub>2</sub> anneal; (2) the P<sub>2</sub> anneal of InAs quantum dots can change the quantum dot morphology remarkably depending on the annealing temperature [12–14]. In this communication, we report our anion exchange approach by improving vertical alignment and island size uniformity in molecular beam epitaxy (MBE)-grown InAs/GaAs dot superlattice structures.

The MBE-grown samples consist of five-layers of two mono-layers (MLs) of InAs, separated by 10 nm GaAs

\* Corresponding authors. Tel.: +1-404-894-8008; fax: +1-404-894-9140.

E-mail addresses: zhong.wang@mse.gatech.edu (Z.L. Wang), april.brown@ee.gatech.edu (A.S. Brown).

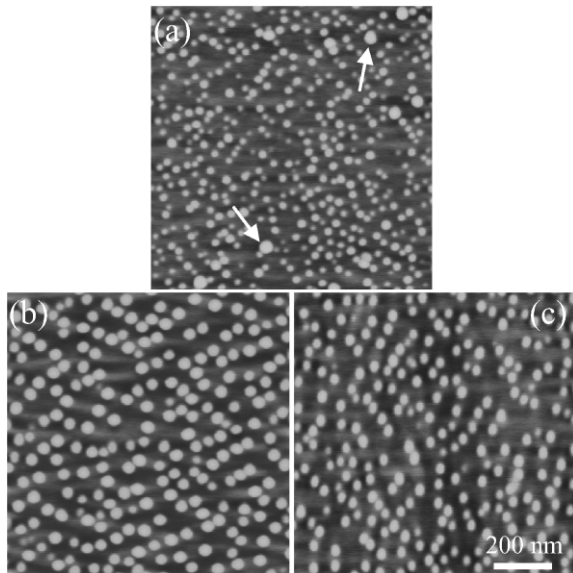


Fig. 1. AFM images of InAs islands. (a) No anneal; (b)  $As_4$  anneal; (c)  $P_2$  anneal.

spacers. The growth temperature of the InAs dots and GaAs layers was 450 °C. The growth rate of the dots was 0.67 Å s. After the formation of InAs islands in each layer, the dot structures were annealed for 3 min at 300 °C either under a  $P_2$  or an  $As_4$  flux. The  $As_4$  beam equivalent pressures (BEP) during InAs growth and anneal were kept the same at  $2.7 \times 10^{-6}$  T. The BEP of the  $P_2$  flux during anneal was  $2.7 \times 10^{-6}$  T. Reflection high-energy electron diffraction was used to monitor the formation of InAs quantum dots. Dot size distribution and density were determined by using atomic force microscope (AFM). Structural features were observed in a JEOL 4000 transmission microscope (TEM) operated at 400 kV.

The AFM images in Fig. 1 illustrate the effect of annealing on the 2 ML InAs morphologies. In Fig. 1(a), the

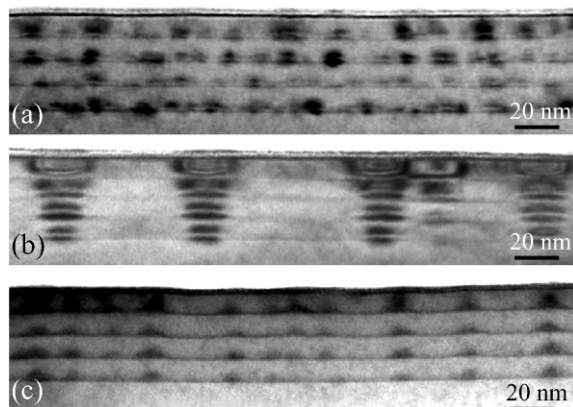


Fig. 2. [110] cross-section TEM images. (a) No anneal; (b)  $As_4$  anneal; (c)  $P_2$  anneal.

InAs islands are not annealed, i.e. the GaAs spacer layers are grown right after the formation of the InAs dots. Clearly, the InAs islands without anneal exhibit a wide size distribution. Quantitative measurement shows that the average island size is 437 nm<sup>2</sup> (diameter, 24 nm), with a standard deviation of 172 nm<sup>2</sup>. The average area density is about  $4.27 \times 10^{10}$  cm<sup>-2</sup>. Fig. 1(b) shows the InAs island morphology after  $As_4$  annealing. As compared with the unannealed dots, the most remarkable change is the increase in dot size (about 1036 nm<sup>2</sup>) and the reduction in area density. Furthermore, the size distribution becomes broader (the standard deviation, 195 nm<sup>2</sup>). This morphological change apparently results from the so-called Ostwald ripening, through which large islands grow at the expense of smaller ones so as to minimize the total energy (surface energy plus elastic strain energy).

In contrast to the  $As_4$  annealing, annealing under  $P_2$  flux produces a much more uniform island size, as shown in Fig. 1(c). It is determined that the average dot size is about 808 nm<sup>2</sup> (diameter, 32 nm) with a much narrow size distribution (standard deviation, 150 nm<sup>2</sup>), and an area density of  $2.62 \times 10^{10}$  cm<sup>-2</sup>.

Fig. 2 shows the [110] cross-section TEM (002) dark field images of the multilayer dot structures. The unannealed islands show poor vertical alignment (Fig. 2(a)). This may result from the weak vertical coupling between the small islands. Generally, islands with size mono-dispersion create a uniform strain template on the spacer layer surface, which provides preferential nucleation and growth, and therefore enhances vertical alignment. The  $As_4$  annealing step produces good vertical alignment (Fig. 2(b)). However, within each column of islands, there is a gradual and remarkable increase in island size with layer number. This vertical size inhomogeneity, along with the in-plane broad size distribution, is apparently a technological disadvantage for  $As_4$  annealing. The  $P_2$  annealing, in contrast, appears to improve both vertical alignment and vertical size uniformity, as shown in Fig. 2(c).

High resolution TEM observation shows that the InAs islands are mostly coherent and misfit dislocations are observed only occasionally in the unannealed and  $P_2$  annealed structures. For the  $As_4$  annealing, however, misfit dislocations are very frequently observed in the upper layer islands, although most of the islands remain coherent in the first two layers.

The advantage of  $P_2$  annealing over the  $As_4$  annealing is further demonstrated in the photoluminescence (PL) spectrum at 4 K, as shown in Fig. 3. The peak width (92 meV) for the  $As_4$  annealed sample is much wider than that of the  $P_2$  annealed (62.5 meV), implying a broader island size distribution for the  $As_4$  annealed sample.

The InAs islands without annealing have smaller size and high area density with broad size distribution and poor vertical alignment. In contrast, the  $As_4$  annealing leads to larger island size with a broader distribution. It improves remarkably the vertical alignment at the cost of vertical size

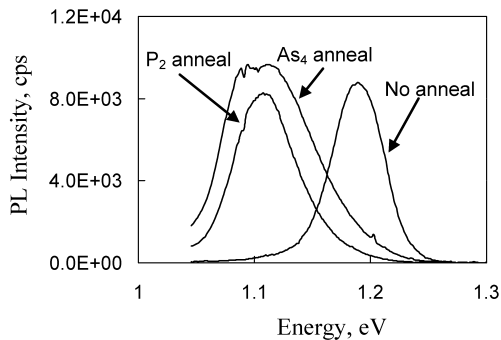


Fig. 3. Photoluminescence spectrum at 4 K.

uniformity. Comparatively, the  $P_2$  annealed islands exhibit both vertical and in-plane size uniformity and good vertical alignment. How can we understand these phenomena?

Energetically, the driving force for the S–K growth is the reduction of the elastic strain energy due to lattice mismatch. It is counter-balanced by the increase in the surface energy. These two forces are temperature insensitive. However, the island size and density are strongly dependent upon growth temperature and rate. Therefore, the island morphology is principally kinetically controlled. This implies that the islands may not be able to develop into their full sizes that are determined thermodynamically. During annealing, this island morphology tends to develop towards the thermodynamically stable morphology.

However, growth of the coherent islands is self-limited or self-organized. To illustrate this point, we need to consider the strain or strain energy distribution around a coherent island. Referring to Fig. 4, the wetting layer far away from the island (region C) experiences the misfit strain  $\varepsilon_0 = (a_{\text{sub}} - a_{\text{epilayer}})/a_{\text{sub}}$ , where  $a_{\text{sub}}$  and  $a_{\text{epilayer}}$  are the lattice constants of the substrate and the wetting layer, respectively. Region A directly beneath the islands is extended and the material in this region is pushed out into region B, which causes an additional strain (to  $\varepsilon_0$ ) or a high strain concentration in the wetting layer along the perimeter of the island, as shown in Fig. 4(b). Correspondingly, there is a peak in the strain energy distribution, as shown in Fig. 4(c). The deep strain or strain energy well along the surface layer of the island is formed due to the strong relaxation (due to less constraint and the transfer of part of the strain energy into region A). The peak in the strain energy distribution forms an energy barrier of height  $E_1$  to the mass transport on the surface. The adatoms from the outside region must overcome this barrier to diffuse onto the island (island growth). In the same way, the atoms also have to overcome a barrier  $E_2$  to diffuse away from the island (island shrinkage). When the island grows larger, the energy barrier increases, and fewer adatoms are able to surpass the barrier. As a result, the growth of the larger islands is decreased in comparison to the smaller ones, narrowing the island size distribution.

Under our growth conditions, the island size is small, and

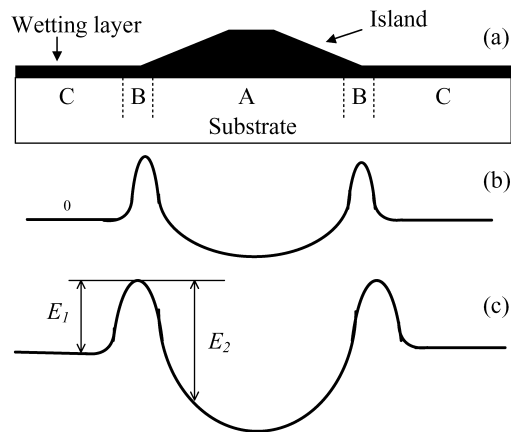


Fig. 4. Schematic diagram of an island structure (a) and in-plane strain (b), and strain energy density (c) distribution along the surface of the wetting layer and island.

hence there is a great amount of surface energy in the dot structure. This causes the dot structure to have a strong tendency towards the thermodynamically stable state. During  $As_4$  annealing, the minimization of surface energy is realized via Ostwald ripening. Due to the self-limiting effect, smaller islands grow faster and hence a narrow size distribution may be expected. However, when the islands grow to a certain size, introduction of misfit dislocations becomes favourable. The growth rate will then be greatly accelerated, resulting in a broadening of the size distribution. Since we frequently observe misfit dislocations in the upper layers islands, we attribute the large size distribution to plastic relaxation. The phenomenon that the island size becomes larger with the stack layer number may be related to the reduction of the critical thickness of the wetting layers [12].

Under  $P_2$  annealing, the P-for-As exchange reaction occurs and forms an  $InP_{(1-x)}As_x$  alloy at the top surface layer of the islands and the wetting layer. This exchange reaction has been shown to be thermodynamically favourable [15]. Furthermore, the lattice constant of the  $InP_{(1-x)}As_x$  is smaller than that of InAs, so the misfit strain energy is reduced, providing an additional driving force for the anion exchange reaction. The P-for-As exchange prefers to occur along the island perimeter, reducing the energy barrier. The exchange in the surface of the wetting layer increases the critical thickness at which the 2D growth mode is switched to 3D growth mode. The reduction of the energy barrier and the increase of the critical thickness decrease the stability of the islands, and enhance the mass transport from the islands to the wetting layer, leading to shrinkage of the islands. Therefore, during  $P_2$  annealing, two opposite processes occur simultaneously. One is island coarsening via Ostwald ripening, and the other is island shrinkage due to anion exchange. At the early stage of annealing, coarsening dominates the whole process and hence the island size grows with annealing time. This explains our

present results. With further annealing, the degree of anion exchange becomes so high that the island shrinks. We have observed complete disappearance of islands under some  $P_2$  annealing conditions [13,14]. Since the higher strain energy barrier favours more exchange, the large islands shrink faster than smaller ones. This is why the P-for-As anion exchange can enhance the size uniformity and vertical alignment.

To summarize,  $As_4$  anneal leads to larger and larger islands via Ostwald ripening. It cannot prevent introduction of misfit dislocations. In contrast,  $P_2$  anneal involves two opposite processes, one is the aforementioned Ostwald ripening, and the other one is anion exchange, which improves vertical alignment and size uniformity and prevent formation of misfit dislocations.

#### Acknowledgments

We gratefully acknowledge the support from the Air Force Research Laboratory under contract F33615-98-C-5428.

#### References

- [1] D. Bimberg, *Semiconductors* 33 (1999) 951.
- [2] C. Pryor, *Phys. Rev. Lett.* 80 (1998) 3579.
- [3] Q. Xie, A. Madhukar, P. Chen, N.P. Kobayashi, *Phys. Rev. Lett.* 75 (1995) 2542.
- [4] G.S. Solomon, J.A. Trezza, A.F. Marshall, J.S. Harris Jr., *Phys. Rev. Lett.* 76 (1996) 952.
- [5] J. Tersoff, C. Teichert, M.G. Lagally, *Phys. Rev. Lett.* 76 (1996) 1675.
- [6] F. Liu, S.E. Davenport, H.M. Evans, M.G. Lagally, *Phys. Rev. Lett.* 82 (1999) 2528.
- [7] S. Rouvimov, Z. Lilliental-Weber, W. Swider, J. Washburn, E.R. Weber, A. Sasaki, A. Wakahara, Y. Furukawa, T. Abe, S. Noda, *J. Electron. Mater.* 27 (1998) 427.
- [8] Y. Furukawa, S. Noda, M. Ishii, A. Wakahara, A. Sasaki, *J. Electron. Mater.* 28 (1999) 452.
- [9] L. Chu, M. Arzberger, G. Böhm, G. Abstreiter, *J. Appl. Phys.* 85 (1999) 2355.
- [10] C. Teichert, M.G. Lagally, L.J. Peticolas, J.C. Bean, J. Tersoff, *Phys. Rev. B* 53 (1996) 16334.
- [11] V. Le Thanh, V. Yam, P. Boucaud, F. Fortuna, C. Ulysse, D. Bouchier, L. Vervoort, J.-M. Lourtioz, *Phys. Rev. B* 60 (1999) 5851.
- [12] J.-J. Shen, A.S. Brown, R.A. Metzger, B. Sievers, L. Bottomley, P. Eckert, W.B. Carter, *J. Vac. Sci. Technol. B* 16 (3) (1998) 1326.
- [13] Y.Q. Wang, J.J. Shen, Z.L. Wang, A. Brown, Structural tuning of InAs/GaAs quantum dots by dissimilar anion annealing, unpublished.
- [14] J.J. Shen, A. Brown, Y.Q. Wang, Z.L. Wang, *J. Vac. Sci. Technol. B* 19 (4) (2001) 1463.
- [15] Y.Q. Wang, Z.L. Wang, T. Brown, A. Brown, G. May, Thermodynamic analysis of anion exchange during heteroepitaxy, *J. Cryst. Growth* (2002) in press.